Thermal instabilities in a mixed convection phenomenon: Nonlinear dynamics

C. Abid and F. Papini
Unité Mixte de Recherche du Centre National de la Recherche Scientifique No. 6595, Institut Universitaire des Systèmes thermiques Industriels, Université d'Aix-Marseille 1, Marseille, France
(Received 16 September 1996; revised manuscript received 30 June 1997)

The influence of mixed convection due to buoyancy for a flow in a uniformly heated horizontal duct is a well-known phenomenon. Experimentally the overall effect of the heating is characterized by a temperature difference between the top and bottom of a cross section. An increase in the average velocity of the fluid or the heating power leads to an instability phenomenon which manifests itself through the appearance of large-amplitude temporal fluctuations in temperature. The amplitude of these fluctuations depends on their position in the test section, the heat flux supplied to the wall and the fluid velocity. The aim of this paper is to describe these thermal instabilities, and to simulate them utilizing a low-dimension model which shows the nonlinear dynamic of the system. [S1063-651X(97)03412-0]

PACS number(s): 47.20.Ky, 47.27.−i

I. INTRODUCTION

The flow in tubes at low Reynolds numbers is a subject of particular significance when heat is transferred through the tube wall. It is encountered in a variety of engineering situations including compact heat exchangers, solar energy collectors, and heat exchangers designed for viscous fluids in the chemical and food industries. Heat is transferred by combined free and forced convection as buoyancy influences become significant.

Many publications (see, for example, Refs. [1–5]) have dealt with mixed convection heat transfer for laminar flow in a horizontal duct. The phenomenon induces a difference in the wall temperature between the top and bottom of the cross section. The secondary motion created in the tube distorts the isothermal parabolic velocity profile, which influences its stability. For a field of values of the flow velocity of the fluid and the heating power at the wall, the wall temperature exhibits strong temporal fluctuations whose amplitudes and occurrence are time varying. These thermal instabilities lead to an intermittent phenomenon. The stability of the flow has attracted the attention of several workers such as in Refs. [6–9], but only Ref. [6] mentioned the intermittency for the wall temperature. Generally, these studies have shown that there exist two types of transitions to turbulence: one of a hydrodynamic nature, the other of a thermal nature; moreover, the presence of secondary flows shifts the transition zone to higher values of the Reynolds number, in relation to the hydrodynamic transition corresponding to the case of the isothermic flow.

The object of the present study is to describe and simulate thermal instabilities of the wall temperature. Experiments were conducted for various values of flow rate and heat flux. A low-dimension model using a modified Hénon mapping is constructed. It is an ''input-output'' model. It allows an intermittent signal similar to the experimental one to be built. Its validation will be carried out by comparing the main characteristics obtained via modeling to those obtained via experimental measurements. This low-dimension ''input-output'' model suggests that this instability is a nonlinear phenomenon which could be described by deterministic dynamics.

II. EXPERIMENTAL EQUIPMENT AND TECHNIQUES

A. Apparatus

A diagram of the heat-transfer loop is shown in Fig. 1. Water from a sump tank circulated through a multistage centrifugal pump (2800 rpm) with a bypass to adjust the flow rate. It flowed through a cooler (heat exchanger) in order to maintain a constant inlet temperature in the system (about 15 °C), to a flow meter, the test section and then the sump tank. The test section consisted of an inconel tube of 10 mm outside diameter and 0.2-mm wall thickness. Electrical cables were connected to its ends through copper flanges to produce Ohmic wall heating. Power from the main supply was controlled using a dc voltage regulator and a variable auto transformer. The heated test section was 100 cm long, preceded by an unheated length of 80 cm to serve as a hydrodynamic entrance region. The density of heat flux P was uniform along the test section, most frequently P

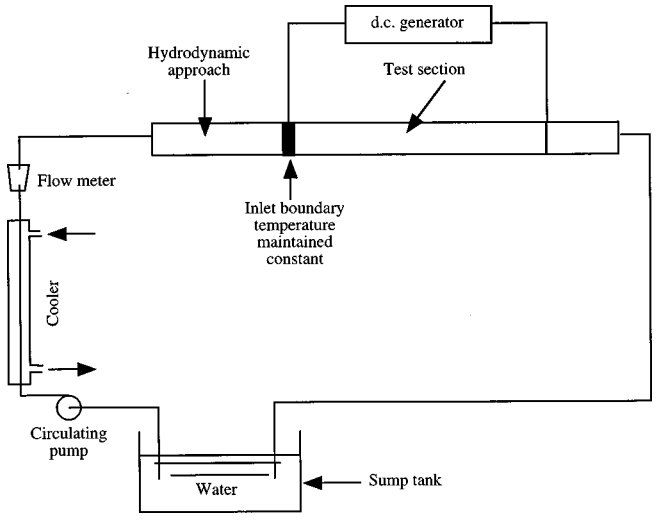

FIG. 1. Diagram of the experimental loop.

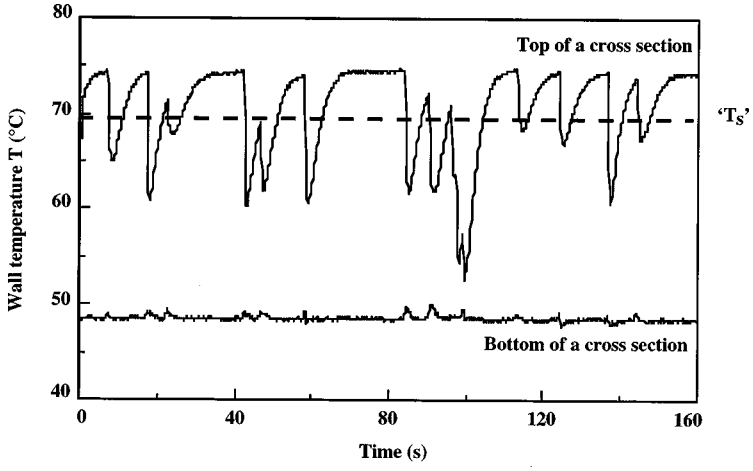

FIG. 2. Wall temperature evolution at the top and the bottom of a cross section $z=80$ cm, $\nu=20$ cm/s (Re=2000), $P=20$ kW/m^2 (Ra=250 000).

$=20$ kW/m^2. The duct was not insulated and so, under these conditions, external heat losses from the duct were approximately about 500 W/m^2. The inlet of the heated zone was taken as the origin of the axial coordinate z.

B. Measuring devices and calibrations

At each axial location z, copper-constantin thermocouples were welded to the top and the bottom sides of the tube, where a temperature difference was created due to buoyancy. All thermocouples were calibrated before being mounted on the loop. Each experiment lasted 7 h. The step of acquisition was about 0.2 s, which led to a recorded signal of 135 000 points.

III. EXPERIMENTAL RESULTS

From experimental observations the temperature of the wall is quasistable, while the Reynolds and Rayleigh numbers (Re and Ra) are low. The properties and characteristics of this flow regime have been described elsewhere [10,11]. It can be noted that the temperature measured at the top of a straight cross section rises when z increases, while at the bottom of this section this value is independent of z; this phenomenon is due to secondary flows, which evolve with the axial coordinate z by transferring the energy supplied to the wall at the bottom of the straight cross section to the upper part of these sections. The transfer coefficient linked to the secondary flows in the lower part of the cross section may also be said to increase with axial coordinate z or the length of time an element of fluid remains in the duct, that is, z/v (where v is the average fluid velocity). Thermal stratification consequently arises in the upper part, in a zone whose area becomes greater as z increases; this follows from the progressive disappearance of transverse velocities. When secondary flows no longer vary (are established), the transfer process in the lower part changes and becomes purely conductive instead of convective; the temperature of the wall at the bottom of the cross section then rises along with that of the top of this section; this occurs for a value of z/v of about 10 s.

Elsewhere [12,13], for adapted coupling of the Reynolds and Rayleigh number values, details of which are given later, an instability is reached for which fluctuations of great amplitude in the wall temperature occur sporadically. Figure 2 presents the wall temperature signal T for the top and bottom of a straight section at axial coordinate $z=80$ cm for a velocity $v=20$ cm/s and a heat flux density $P=20$ kW/m^2. The top of the duct cools down very quickly with a time constant of about 2 s, and then it returns to the steady state with a time constant of about 10 s. The amplitude of the peak is time varying. The duration of the steady-state phases are also time varying. In addition, when the cross section is scanned around its circumference, the amplitude of the fluctuations varies from its maximum at the top of the cross section to its minimum at the bottom. The phenomenon thus characterized will be called ''intermittent.'' It is noteworthy in Fig. 2 that there is a particular behavior in which the fluctuations do not allow the steady state to be attained in the time interval separating the fluctuations, if they are too close in time. This property will be called ''turbulence associated with intermittence.''

A. Evolution of signals versus axial coordinate

Furthermore, a study of the temperature signals corresponding to simultaneous records at different z coordinates shows the propagation of the instability. The propagation velocity calculated from the intercorrelation functions of the signals is close to the average fluid velocity. Passing from one coordinate to another is statistically expressed only by an increase in the amplitude of the fluctuations according to the variation of the temperature difference between the top and bottom of a cross section. In order to define this evolution, a signal analysis procedure was used, which consisted in assessing the number n of time intervals for which $T>T_s$, with T_s a temperature threshold which is made to vary with a ΔT_s step (see the Appendix and Fig. 2). Figure 3 displays the n versus T_s diagrams corresponding to these signals for a given values of Ra and Re. It can be noted that an increase in the axial coordinate corresponds to a more well-defined zone where the number of phases is constant, and where there is no new peak minimum. This zone corresponds to what we call a forbidden gap. Thus the evolution versus the axial coordinate is characterized by the evolution of the width of the forbidden gap, which becomes larger and larger. Thus for

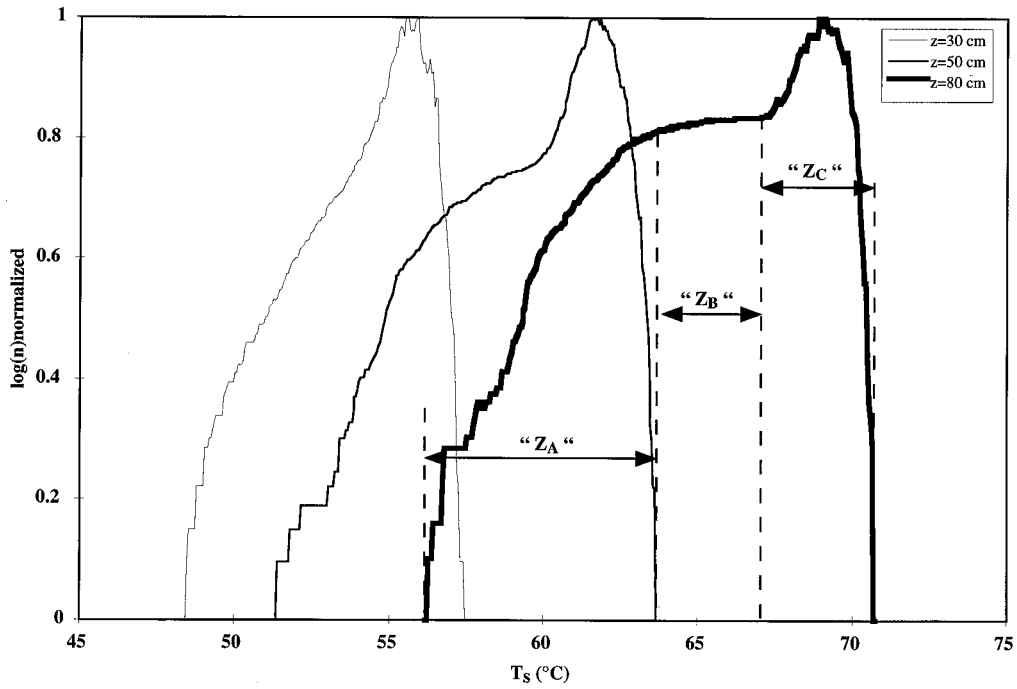

FIG. 3. Diagram $\log(n)$ (normalized value) vs T_s of the wall temperature for various axial coordinates z. Re=2000, Ra=200 000.

$z=80$ cm, three well-defined zones can be observed: Z_A, characterized by peaks of large amplitude; Z_B, characterized by the forbidden gap; and Z_C, characterized by the steady state.

In fact, when a fluctuation occurs at location z, the thermal configuration at the peak minimum is close to the thermal and hydrodynamic configurations of the steady state for a coordinate z' smaller than the observation coordinate z (this configuration will be called the solution in z'). This has been confirmed by measurement of the spatiotemporal distributions of temperatures on the outer surface of the duct wall. It acts as if the system were joining a coordinate z' smaller than z. As the amplitude of the peak varies, the z' value varies from one peak to another. The various solutions z' belong to the same laminar state, which means that the system evolves in the same space of solutions, that is, the laminar solutions. Actually, statistically, everything acts as if a fluid element remains in the same state, as from axial coordinate z', when conveyed inside the duct. Thus, at observation coordinate z, the solution defined and fixed in z' will be recorded. The existence and progressive widening of the forbidden gap simply show that the fluctuations arise near the inlet of the heated zone, to be subsequently conveyed and structured during their displacement in the duct.

In order to study this intermittent phenomenon, characterized and identified by the temperature fall and rise time constants and the presence of the forbidden gap, the time signal which corresponds to the temperature of the outer wall, at the top of the straight cross section for axial coordinate $z=80$ cm, will be considered in particular.

B. Influence of the fluid velocity and the heating power

Flow stability could be influenced by two independent parameters: flow rate and heating power. Two series of tests were performed to examine the influence of each parameter separately; for tests of each series, one parameter was kept constant while the other was gradually increased.

In the first series of tests the fluid velocity was kept constant, and the heating power was made to vary, which amounts to varying the Rayleigh number (Ra is calculated using the difference of the fluid temperature between the inlet and the exit of the duct). As an illustration, Fig. 4 represents the evolution of the wall temperature for different values of the Rayleigh number, obtained for a value of Reynolds number of 900. For the lowest value of the Rayleigh number, it may be seen that the temperature signal is quasistable; progressively, when this parameter increases (that is, the heating power increases) the signal becomes intermittent; the number of fluctuations per time unit subsequently increases with the control parameter value. A greater increase in this value leads to thermal turbulence, which is the case of the signal represented with the highest value of Ra.

In the second series of tests the heating power was kept constant, and the flow velocity of the fluid was made to vary. Figure 5 shows the evolution of the wall temperature for various Reynolds number values, for a given heating power value. It can be seen that the wall temperature signal is quasistable, for the lowest value of Re; when this parameter increases (that is, the average velocity of the fluid increases) the signal progressively becomes intermittent, and the number of fluctuations per time unit increases with the value of the control parameter. A greater increase in this value leads to hydrodynamic turbulence, which is the case for the signal represented with the highest value of Re.

A stability pattern (Fig. 6) was determined from these results in the (Re-Ra) plane, and the zone corresponding to the intermittent signal was identified. In the field of the intermittence the temperature fall and rise time constants are maintained; the increase in Ra or Re corresponds to an increase in the number of fluctuations.

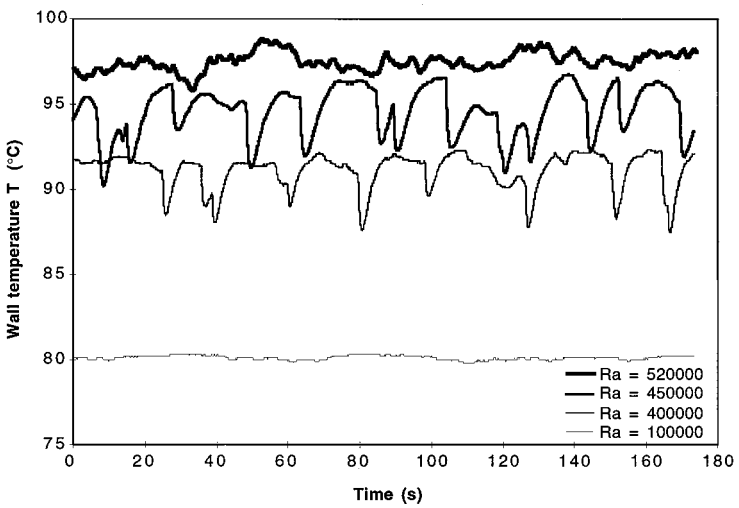

FIG. 4. Wall temperature evolution vs Rayleigh number. Re=900, $z=80$ cm.

From a physical point of view, the intermittent phenomenon is set off by low-amplitude primary instability of thermal and/or hydrodynamic origin. The large-amplitude instability (fluctuations of the wall temperature) results from a mechanism which is intrinsic to mixed convection, created by the competition between two effects.

(i) The first is a destabilizing effect related to the axial flow. Buoyancy and concomitant secondary flows distort the longitudinal velocity profile. The latter tends to an axially symmetric profile which is more logical with the cylindrical geometry. This induces an increase in the longitudinal velocities at the top of a cross section and an increase in the heat transfer, with a sudden decrease in the local temperature.

(ii) The second stabilizing effect is associated with the secondary flow, which is maintained via the buoyancy effect and wall heating.

It can also be said that the return to a Poiseuille-type profile corresponds to a change in the heat-transfer process in the straight cross section, in particular in the lower part of these sections. There is a change from a convective mode to a conductive mode. In the former case, heat supplied at the lower part is convected to the upper part of the section by secondary flows, while in the latter case this heat is convected by the main flow and diffused to the inside of the section; during this transformation, there is a modification of the structure of the secondary flows, causing the destruction of the thermal stratification in the upper part, that is, the cooling of the fluid and the wall (at this point). This rapid change in behavior is possible when the time characteristics of the two transfer modes are sufficiently close, which is the case with water, with a Prandtl number of around 6. It is no longer the case when this number increases, which could be seen for a water-glycol mixture, for which there no longer

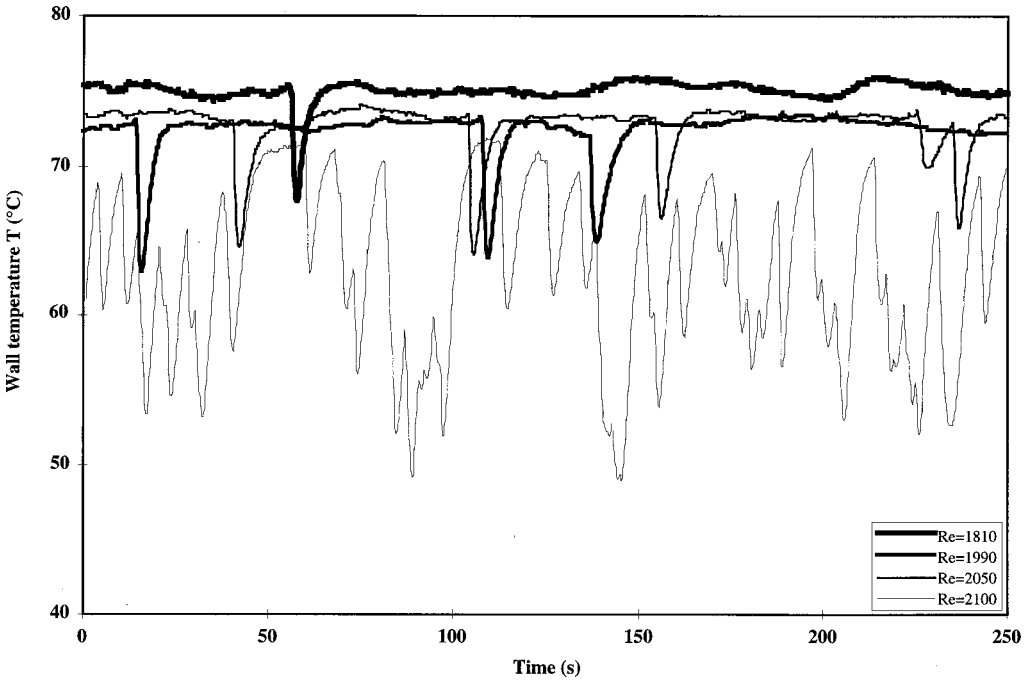

FIG. 5. Wall temperature evolution vs Reynolds number. Ra=200 000, $z=80$ cm.

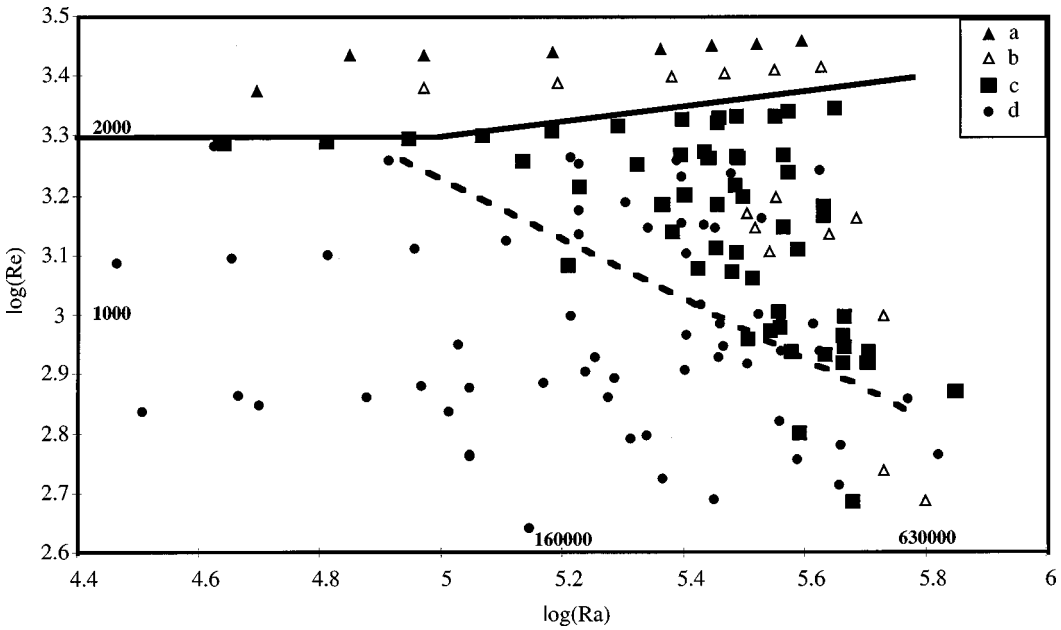

FIG. 6. Diagram of stability of the system: log(Re) vs log(Ra) $z=80$ cm. (a) Turbulent signal. (b) Mixed ''intermittent-turbulent'' signal. (c) Intermittent signal. (d) Quasistable signal.

exist great amplitude fluctuations at the wall, under the same conditions. This description of the mechanism is confirmed by the fluid temperature measurements in the cross section [14].

The two stabilizing and destabilizing effects are in fact coupled, since the distortion of the axial longitudinal profile of velocity is linked to the maximum difference of temperature between the top and bottom of a cross straight section; thus the notion of nonlinearity is introduced when working out a low-dimension model which simulates the intermittence phenomenon.

IV. DESCRIPTION OF THE PHENOMENON WITH A NONLINEAR MODEL: HÉNON MAPPING

The modeling which is proposed is a low-dimensional one. It could be considered to generate solutions which express the evolution of the physical signal for the wall temperature measured at the top of the duct at a given cross section. This model is nonlinear, and operates by iteration within a limited span of solutions. Moreover, time constants of the problem (the fall and rise of the temperature) are not generally taken into account, so that the results will be obtained according to a dimensionless time; these time constants are effectively the only parameters which enable a physical time scale to be fixed. The statistical distribution of the amplitude of fluctuations through a deterministic description will therefore be the object of interest.

An intermittent signal can be considered to be the result of alternating between ''A'' and ''B'' sets of solutions. Set A corresponds to the steady state, and set B to the peak minimum. If both sets belong to the same state or space, a mathematical transformation Λ exists such that Λ is a mapping of the space of X solutions on itself. It is an iteration on k according to:

$$X_{k+1}=\Lambda(X_k,X_{k-1},\ldots).$$

The following nonlinear discrete equation, corresponding to a Hénon mapping which iterates on k, can describe the phenomenon

$$X_{k+1}=1-cX_k^2+dX_{k-1},$$

where c is the first Hénon mapping constant ($c=1.4$), and d is the second Hénon mapping constant ($d=0.3$). The structure of a Hénon mapping is a two-dimensional representation of a Lorenz model and a simplification of the Navier-Stokes equations [15].

For each value i of discrete time, a new fluid element is considered to reach a location z. Each fluid element is subjected to the same evolution when passing into the heated duct from the inlet as far as the coordinate z. In addition, state A seems to be more stable since it persists for a longer duration (steady phases). The steady phase durations are time varying. For each value i, the stability of solution A and the forbidden gap will be taken into account by introducing a constraint S_t which brings back to A any solution B not far enough from A. S_t also represents the width of the forbidden gap. This mapping is such that

$$X(i,k+1)=1-cX(i,k)^2+dX(i,k-1),$$

$$S-S_t<X(i,k+1)<S\Rightarrow X(i,k+1)=S+g(i),$$

where S corresponds to the quasistable state, and its value is taken equal to 0.7; it represents the approximate value of the unstable fixed point of the map.

The input magnitude, which varies according to time, is noise, whose structuration (by the modified Hénon operator which has been defined) is therefore to be examined. It is to be noted that the problem of the structuration of an external noise, in an intermittent signal, has been studied elsewhere by using the generic Ginsburg-Landau equation [16,17]. In the case of our study, the input conditions are

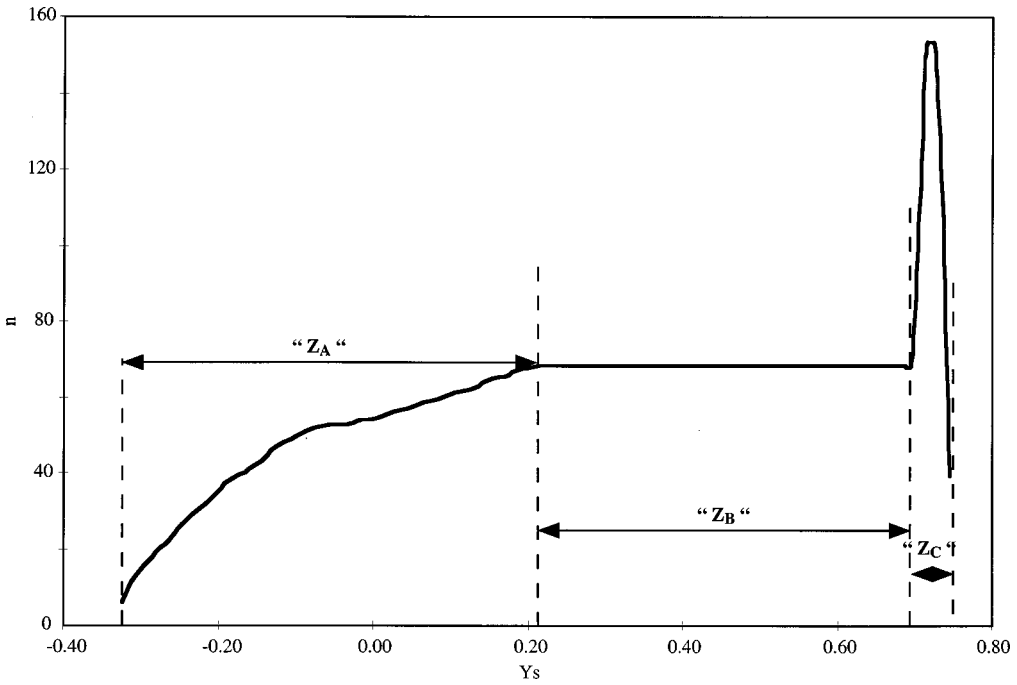

FIG. 7. Diagram n vs Y_s of the modeled signal. $S_t=0.22$.

$$X(i,0)=S+g_0(i) \quad \text{and} \quad X(i,1)=S+g_1(i),$$

where $g(i)$, $g_0(i)$, and $g_1(i)$ correspond to random series with values included in the interval [0; 0.05], by generally assuming $g=G/m$, where G is a random number, between 0 and 1 and m an integer number above 1.

The value of k is such that: $0<k<k_{\max}$, and it corresponds to the iteration scheme which allows the unstationary solutions of the Hénon mapping to be bypassed, and the constraint effect to be taken into account better. For the calculations, a value of $k_{\max}=30$ was considered, beyond which the results were no longer varied.

The time signal is built by the successive output solutions $Y(i)$, such that $Y(i)=X(i,k_{\max})$. The solutions obtained are dimensionless. Figure 7 displays the $n=f(Y_S)$ diagram (number of phases or time intervals versus the threshold value Y_s corresponding to Y). It is noted that the intermittent behavior is simulated by this model well. As in Fig. 3, zones Z_A, Z_B, and Z_C can be observed.

Now just the Z_A zone is considered in order to study the distribution of the peaks. The curves of Fig. 8 display $N=f(L)$ for the experimental signal for various ΔT_s scales (see the Appendix for the calculation and definition of N and L). Figure 9 shows the same results produced by the Hénon mapping. The comparison of both results shows that the Hénon mapping which is initiated by low-amplitude noise leads to fine structures which are similar to the experimental ones.

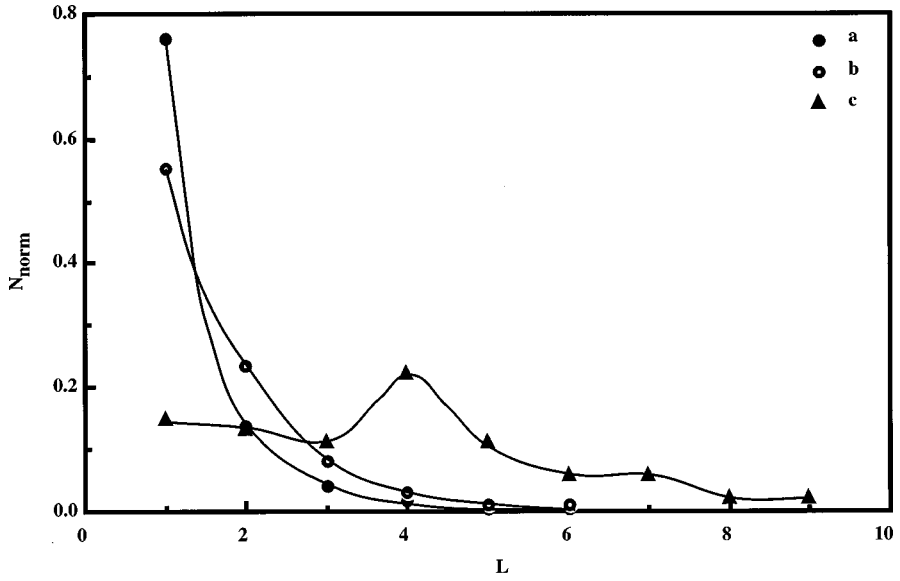

FIG. 8. Diagram: N vs L for an experimental signal. The normalized value of N (N_{norm}) was represented. (a) $\Delta T_s=0.0025$ °C. (b) $\Delta T_s=0.05$ °C. (c) $\Delta T_s=0.2$ °C.

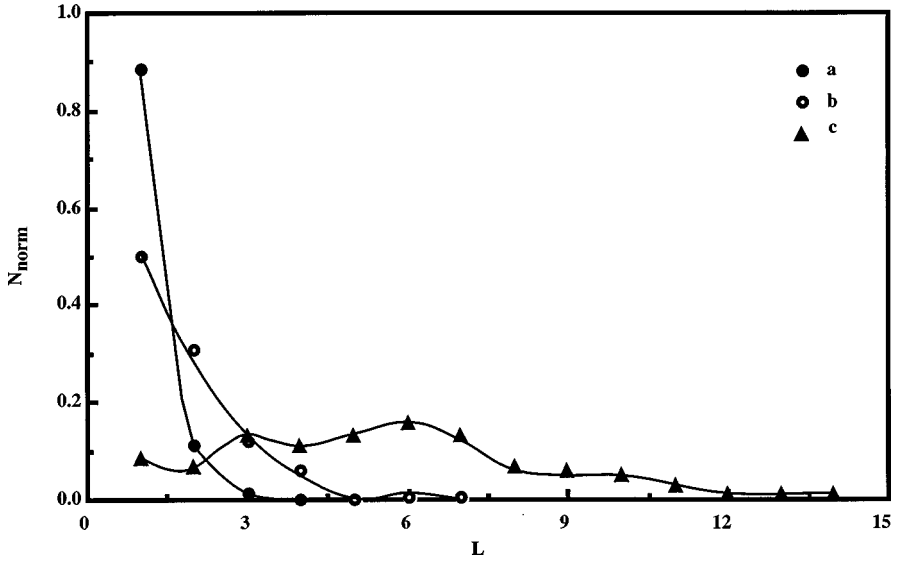

FIG. 9. Diagram: N vs L for a modeled signal. The normalized value of N (N_{norm}) was represented. (a) $\Delta Y_s = 0.0005$. (b) $\Delta Y_s = 0.0025$. (c) $\Delta Y_s = 0.01$.

In this part, the Hénon mapping was considered to generate solutions at location z. This model could be improved if it takes into account the time constants associated with the fall and rise of the wall temperature. In this case, the phenomenon, which we have called turbulence associated to intermittence, may be found, when solutions of the model are generated during the phase corresponding to a temperature rise. In the following it will be shown how the various control parameters act in such a low-dimension model.

V. ANALYSIS OF EXPERIMENTAL AND MODELED SIGNALS

A. Effect of the axial coordinate

Referring to Fig. 3, it can be seen that the forbidden gap disappears when the value of z decreases or more exactly, it forms when z increases. This disappearance may be attributed to pollution of the forbidden gap such that, statistically, more and more solutions may enter it; this actually depends on the statistical law of creation of the fluctuations in the zone near the duct inlet (which is difficult to determine experimentally, the fluctuations being drawn from a noise sig-

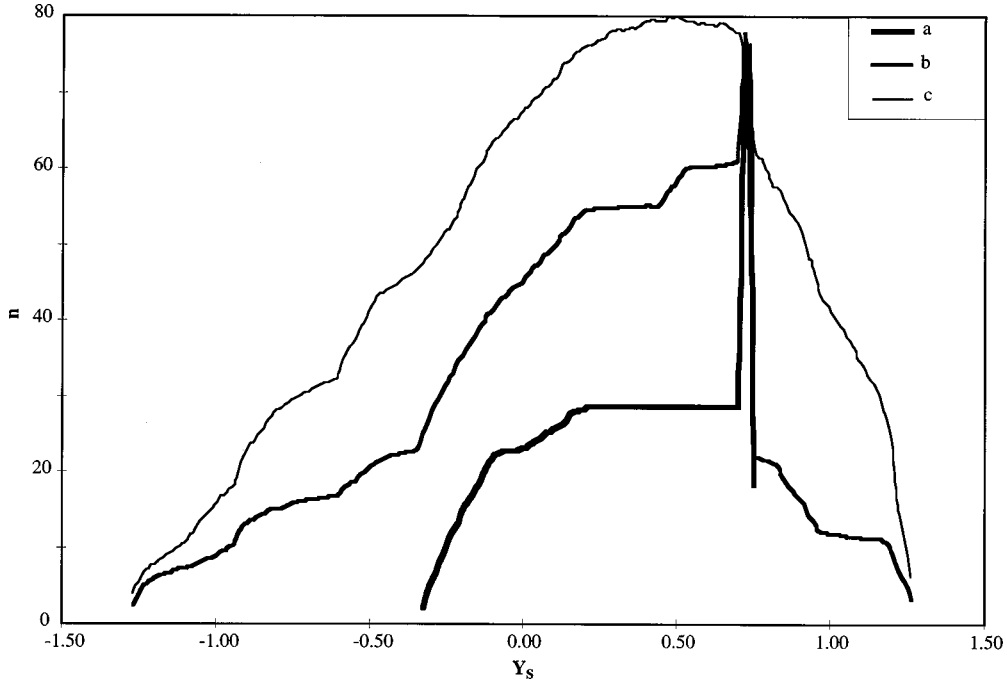

FIG. 10. Diagram n vs Y_s of the modeled signals for various probabilities of the pollution of the forbidden gap. (a) $p = 0$. (b) $p = 0.095$. (c) $p = 0.5$.

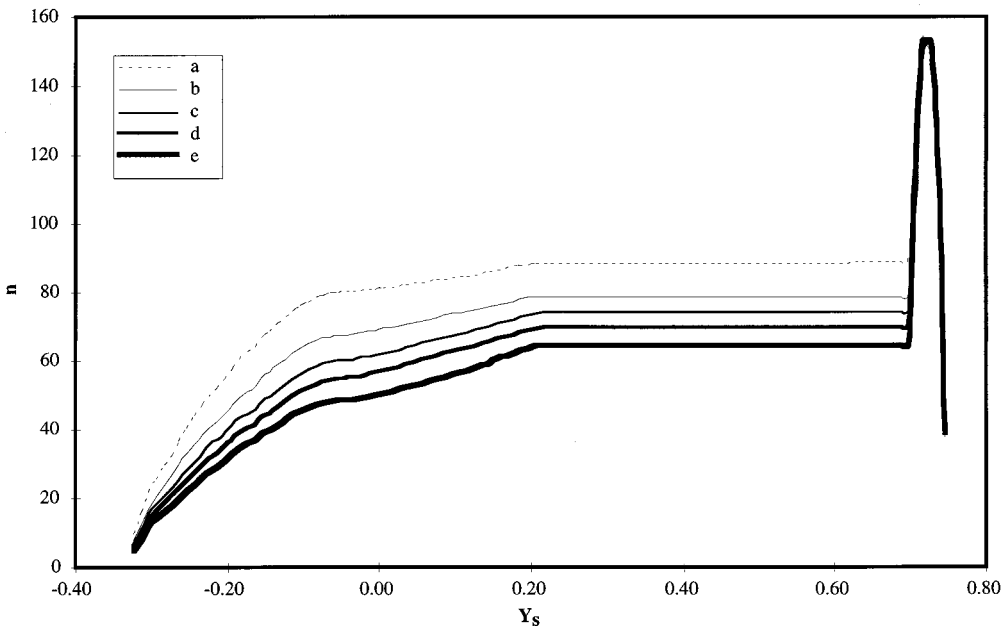

FIG. 11. Diagram n vs Y_s of the modeled signals for various amplitudes of the noise (for the input conditions) corresponding to various values of the parameter m. (a) $m=10$. (b) $m=15$. (c) $m=17$. (d) $m=19$. (e) $m=22$.

nal). Simulating the behavior for axial coordinates closer to the inlet of the heated zone is tantamount to deteriorating the forbidden gap; this deterioration consists in introducing a law of probability p of the presence of fluctuations in the forbidden gap. To simplify, this law will be taken as uniform and is considered during the iteration scheme such that

$$S-S_t<X(i,k+1)<S \quad \text{and} \quad G<p \Rightarrow X(i,k+1)=S+g(i),$$

where G is a random number. Thus Fig. 10 shows the distribution functions of signals obtained for different pollution probability functions of the forbidden gap. It may effectively be noted that the forbidden gap forms when the probability of the presence of a solution decreases. Qualitatively, this evolution reflects the behavior of the distribution functions in relation to axial coordinate z.

B. Effect of the fluid velocity and the wall heating

The increase in the Reynolds and Rayleigh numbers, in the area where the signal is intermittent, corresponds to an increase in the number of fluctuations in the signal; this may be interpreted by stronger and stronger primary instability

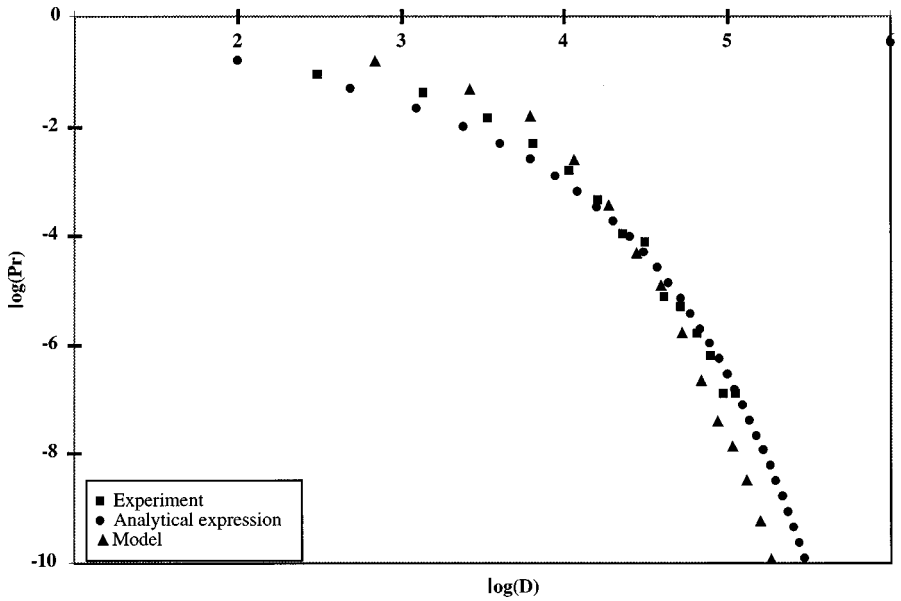

FIG. 12. Probability of number of phases which have a duration above a certain duration D. Comparison between the experimental and modeled signals with the analytical expression.

when these two parameters increase. The model that we have elaborated takes into account the primary instability which is to be found in the input condition as a noise of finite amplitude superimposed on a stationary signal. The effect of an increase in the Reynolds or Rayleigh number may then be simulated by superimposing a greater and greater amplitude noise on the stationary signal. Thus Fig. 11 shows the $n = f(Y_s)$ diagram of signals obtained for different values of the noise amplitude. The increase in noise amplitude at the inlet significantly affects the increase in the number of fluctuations in the signal. This is therefore in agreement with the evolution of the phenomenon in relation to the Reynolds and Rayleigh numbers.

VI. STATISTICS OF LAMINAR PHASES

Finally, Fig. 12 shows the statistics of the temporal distribution of the steady or laminar phases for the experimental and the modeled signals. The shape of the curves is then typical of a type-III intermittence phenomenon, as demonstrated by the comparison with the analytical expression of this type of intermittence [15].

VII. CONCLUSION

The description of the temporal dynamics of the large-amplitude instabilities in our experiments was modeled without the introduction of a model of hydrodynamic turbulence. A primary instability of thermal or hydrodynamic nature is considered to be at the origin of this intermittent phenomenon. It can be associated with an inflection in the profile of longitudinal velocities or a Tollmien-Schlichting instability [18–20], with a fluid whose Prandtl number is close to the unity.

An ''input-output'' model based on a Hénon mapping associated with a constraint on the steady state has enabled the main experimental characteristics of the phenomenon (fine structures, forbidden gap, turbulence associated with intermittence, statistics about the durations of steady phases) to be simulated. This model is a reduction of a three-dimensional and complicated system. Intermittent signals have therefore been obtained from an input noise of infinitesimal amplitude structured by Hénon mapping (sensitivity to the initial conditions). The scheme agrees with an intermittence of type III. The phenomenon is described by a nonlinear dynamic. This simplified low-dimension model enables the main characteristics of the physical phenomenon to be found through a behavior model.

ACKNOWLEDGMENT

Professor R. Sani (University of Colorado) is gratefully acknowledged for constructive discussions.

APPENDIX: DESCRIPTION OF THE ANALYSIS TOOL

The temperature signatures are included in a temperature interval defined by upper and lower boundaries. The upper boundary corresponds to the steady state, and the lower boundary to the lowest temperature attained by fluctuations. For an intermittence phenomenon, the statistics of the durations for which the measurement is above a given threshold value T_s are generally considered (see Fig. 2). The variation (with a step ΔT_s) of this threshold value enables statistics concerning the amplitude of the fluctuations to be generated.

For each T_s value, the number of durations (or number of phases) n for which the temperature is above T_s will be counted. It is obvious that the duration of these phases is time varying. One can also define a function Δn as

$$\Delta n = [n(T_s + \Delta T_s) - n(T_s)]/\Delta T_s .$$

Δn is a multiple of $1/\Delta T_s$ (this last number representing an observation scale factor), so we can write:

$$\Delta n = L \Delta T_s .$$

In order to bypass the parameter T_s, another representation can be obtained by tracing the discrete diagram Δn versus n. To each value Δn corresponds N different values of n; then we can simplify the exploitation of these data, and so plot the diagram $N = f(L)$. As an illustration, for a signal generated from the drawing of random numbers uniformly distributed on the interval 0–1, the diagram $N = f(L)$ is flat whatever value ΔT_s. So, any significant difference in the behavior from the random one denotes a more complex distribution and the existence of ''fine structures.''

[1] R. L. Shannon and C. A. Depew, ASME J. Heat Transf. **90**, 353 (1968).
[2] A. E. Bergles and R. R. Simonds, Int. J. Heat Mass Transf. **14**, 1989 (1971).
[3] P. H. Newell, Jr. and A. E. Bergles, ASME J. Heat Transf. **92**, 83 (1970).
[4] S. V. Patankar, S. Ramadhyani, and E. M. Sparrow, ASME J. Heat Transf. **100**, 63 (1978).
[5] D. Choudhury and S. V. Patankar, ASME J. Heat Transf. **110**, 901 (1988).
[6] P. S. Petukhov and A. F. Polyakov (unpublished).
[7] H. R. Nagendra, Fluid Mech. **57**, 269 (1973).
[8] M. A. El-Hawary, Int. J. Heat Mass Transf. **102**, 273 (1980).
[9] S. Bilodeau, N. Galanis, and A. Laneville (unpublished).
[10] C. Abid, Ph.D. thesis, Marseille, 1993.
[11] C. Abid, F. Papini, A. Ropke, and D. Veyret, Int. J. Heat Mass Transf. **37**, 91 (1994).
[12] C. Abid, F. Papini, and A. Ropke, J. Phys. III **3**, 255 (1993).
[13] C. Abid, F. Papini, and A. Ropke, Int. J. Heat Mass Transf. **38**, 287 (1995).
[14] C. Abid and F. Papini (unpublished).
[15] P. Bergé, Y. Pomeau, and Ch. Vidal, *L'ordre Dans le Chaos* (Hermann, Paris, 1988).
[16] R. J. Deissler, Physica D **25**, 233 (1987).

[17] R. J. Deissler, J. Stat. Phys. **54**, 1459 (1989).
[18] H. Schlichting, *Boundary-Layer Theory*, 2nd ed. (McGraw-Hill, New York, 1979).
[19] E. Guyon, J. P. Hulin, and L. Petit, *Hydrodynamique Physique. Savoirs Actuels* (CNRS, Paris, 1991).
[20] A. S. Monin and A. M. Yaglom, in *Statistical Fluid Mechanics: Mechanics of Turbulence*, edited by J. L. Lumley (MIT Press, Cambridge, 1979).